Anisotropic Thermal Expansion of Tetragonal Zirconia Polycrystals

Tzer-Shin Sheu[*,†]

Department of Materials Science and Engineering, The University of Michigan, Ann Arbor, Michigan   48109-2136

Thermal expansion coefficients (α_a and α_c) in two crystallographic axes (a and c) of the tetragonal phase are measured at 25°-1200°C in $ZrO_2-M_2O_3$ (M = Sc, In, Yb) and in ZrO_2-YTaO_4. The difference between these two thermal expansion coefficients, $\alpha_c - \alpha_a$, decreases with M_2O_3 or $YTaO_4$ composition even though the tetragonality (c/a) behaves differently in these two systems. The locus of $\alpha_c = \alpha_a$ represents a maximum tetragonality for the tetragonal phase, but not the phase boundary for the cubic phase. The relationships among thermal expansion, temperature, and composition are discussed.

I. Introduction

DIVALENT and trivalent metal oxides such as MgO, CaO, Y_2O_3, and rare-earth oxides have been found to be the stabilizing agents in zirconia solid solutions.[1,2] This is because the tetragonal phase (t) decreases both its tetragonality (c/a) and its transformation temperature to the monoclinic phase (m) by adding these oxides to the pure zirconia.[3-6] Conversely, pentavalent metal oxides such as Ta_2O_5 and Nb_2O_5 act as destabilizers,[6,7] because these oxides increase both the tetragonality and the transformation temperature of $t \rightarrow m$ when they are added to the 2 or 3 mol% Y_2O_3-tetragonal zirconia polycrystalline material (TZP). Therefore, it is generally believed that the transformation temperature of $t \rightarrow m$ is correlated with tetragonality.

However, the above correlation does not exist in the ZrO_2-YTaO_4 system, whose isothermal ternary oxide phase diagram at 1500°C is shown in Fig. 1. A stable tetragonal phase with a tetragonality larger than that in the pure zirconia has been reported to exist in the composition range 15-25 mol% $YTaO_4$ at 25°C.[7] With composition less than 14.0 mol% $YTaO_4$, $t \rightarrow m$ transformation temperature decreases with increasing $YTaO_4$ composition. This suppression of $t \rightarrow m$ transformation temperature indicates that $YTaO_4$ oxide is a stabilizing agent. However, there is no strong evidence to prove whether the unquenchable tetragonal phase with 0-14 mol% $YTaO_4$ has the same crystal structure as the stable tetragonal phase with 15-25 mol% $YTaO_4$. In this study, a lattice parameter measurement at high temperature is used to investigate the phase continuity in the composition range 0-25% $YTaO_4$.

Anisotropic thermal expansion behavior ($\alpha_c \neq \alpha_a$) has been reported to affect tetragonality (c/a) for the tetragonal zirconia crystals,[8-10] where α_a and α_c are thermal expansion coefficients for the crystallographic a and c axes, respectively. In the $ZrO_2-Y_2O_3$ system, c/a and α_c/α_a are temperature-dependent, and both of them decrease as Y_2O_3 composition increases at temperatures of 25°-800°C.[8] In the pure zirconia, c/a first increases and then decreases as temperature increases from ~1100°C up to ~2370°C.[9] This reverse c/a behavior also exists in the t'
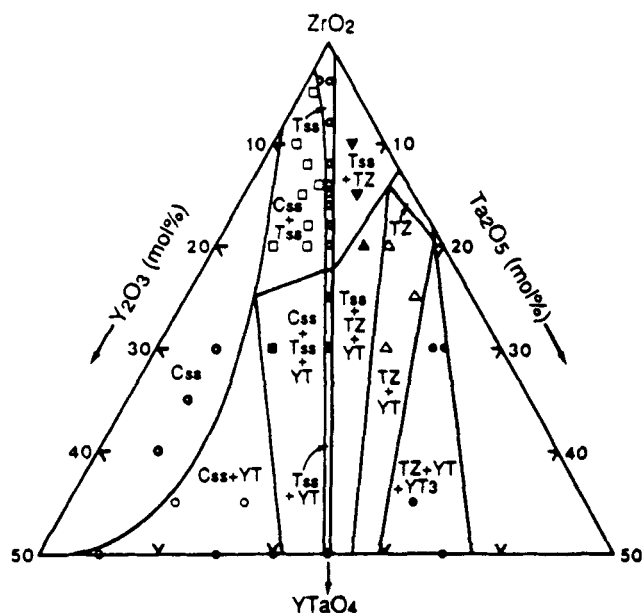
Fig. 1. Part of the ternary phase diagram for the system $ZrO_2-Y_2O_3-Ta_2O_5$ at 1500°C. Tss is t-ZrO_2 solid solution, Css is c-ZrO_2 solid solution, TZ is $Ta_2Zr_6O_{17}$, YT is $YTaO_4$, YT_3 is YTa_3O_9 (Ref. 7).

phase,[10] which is the product of the diffusionless phase transformation from the cubic phase to the tetragonal phase. The maximum c/a is shifted to a lower temperature as Y_2O_3 composition increases. Based on these temperature- and composition-dependent tetragonality curves in the $ZrO_2-Y_2O_3$ system, the anisotropic thermal expansion of the tetragonal phase will be discussed in this study. In the ZrO_2-YTaO_4 system, the tetragonal phase shows some interesting phenomena for its tetragonality and its $t \rightarrow m$ transformation temperature. Its anisotropic thermal expansions will be measured to compare with those in the $ZrO_2-M_2O_3$ (M = Y, Yb, In, Sc) systems.

II. Experimental Procedure

Different compositions of tetragonal zirconia polycrystalline materials were produced by making fine powder, sintering, and heat-treating. Fine powder was prepared from precursor metal hydroxide using a coprecipitation method. Starting materials were 99.9% pure M_2O_3 (M = Y, Yb, In, Sc), 99.9% pure Ta_2O_5, and 93.1% pure $ZrOCl_2-8H_2O$ (the remaining balance is H_2O). M_2O_3 and Ta_2O_5 were dissolved in hot acid (HCl or HNO_3), and $ZrOCl_2-8H_2O$ was dissolved in distilled water. Two solutions, containing M^{+3} (or Ta^{+5}) plus Zr^{+4} and NH_4OH (10 wt%), were added simultaneously and mixed together to let a gellike metal hydroxide precipitate out by controlling the pH value above 9. Precipitate was separated by filtration and was washed with water to eliminate chlorine ions. Then it was dried in an oven at 80°C. Dried precipitates were calcined in an air oven for 2 h at 650°C. Pellets were formed under a uniaxial pressure and were then isostatically pressed at 340 MPa. Subsequently, green pellets were sintered and heat-treated in air in a furnace with $MoSi_2$ heating elements.

For the lattice parameter measurement, samples in either a sintered powder or pellet form were used. Diffraction patterns of these samples were obtained using a high-temperature X-ray diffractometer (Geigerflex, Rigaku, Tokyo, Japan). An Al_2O_3 plate was used as a sample holder and as an internal standard to calculate the lattice parameters. The reference diffraction peaks of Al_2O_3 were calibrated by pure Pt powder. The lattice constants of pure Pt metal at different temperatures were calculated from the thermal expansion data published by the National Bureau of Standards[12] and from the Pt lattice constant at room temperature shown in JCPDS card number 4-802. Transformation temperatures between the tetragonal and the monoclinic phases were measured by a dilatometer unit. The operating temperature range was 25°–1300°C; heating and cooling rates were 10°C/min.

III. Results

(1) Phase Continuity in the Composition Range 0–25 mol% $YTaO_4$

A sample with 13.0 mol% $YTaO_4$ contains both the tetragonal phase and monoclinic phase at room temperature. Its phase evolution at high temperatures is shown in Fig. 2. The characteristic monoclinic and tetragonal peaks $(11\bar{1})_m$, $(111)_m$, $(111)_t$, $(004)_t$, and $(400)_t$ are used to identify these two phases. At 600° and 900°C, the tetragonal phase and the monoclinic phase coexist. At 1200°C, only the tetragonal phase exists. This phase evolution indicates that the monoclinic phase at low temperatures is progressively transformed into the tetragonal phase at high temperatures. The same phase evolution is also found in the samples with composition less than 13.0 mol% $YTaO_4$. The diffraction peaks in Fig. 2 shift to the low 2θ angle as the temperature increases, due to the larger lattice constants at high temperatures.

At 1200°C, only the tetragonal phase is present in the composition range 0–25 mol% $YTaO_4$. Its lattice constants versus composition are shown in Fig. 3. Both lattice constants c and a are linearly dependent on composition. Figure 3 also shows the relationships between lattice constants and composition at 25°C. Lattice constants for samples with composition less than 14.0 mol% $YTaO_4$ are obtained from data at high temperatures by using an extrapolation method, because the tetragonal phase is unstable at room temperature. A linear regression method indicates that pure tetragonal zirconia has lattice constants $a =$
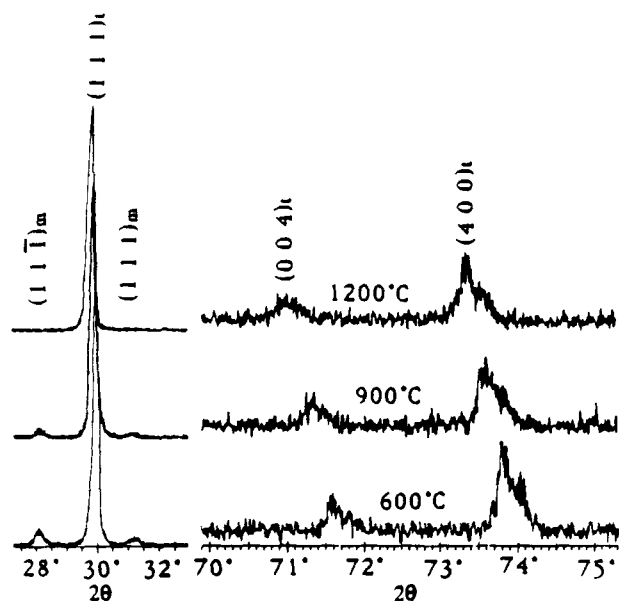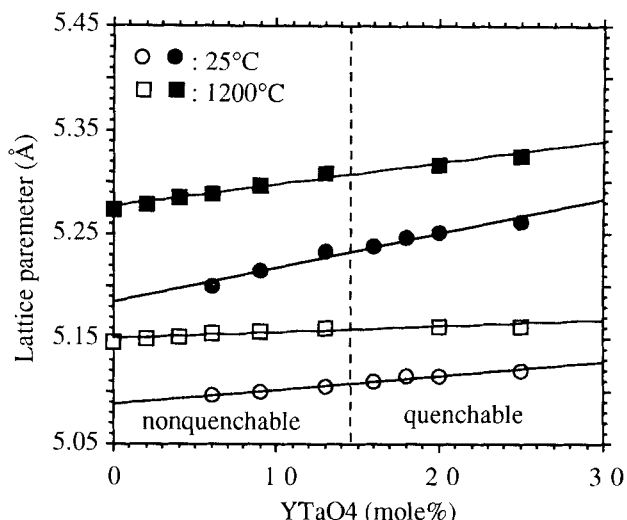

Fig. 3. Lattice parameters at 25° and 1200°C. Open symbols are for lattice constant a and closed symbols are for lattice constant c.

5.0887 Å and $c = 5.1849$ Å at 25°C, which is consistent with previous data.[3,4] Based on the above lattice constant continuities at 1200°C and at room temperature, it is suggested that only one tetragonal phase exists in the composition range 0–25 mol% $YTaO_4$.

(2) Tetragonality and Anisotropic Thermal Expansion Coefficients

Tetragonality (c/a) in the ZrO_2–$YTaO_4$ and ZrO_2–M_2O_3 systems at 1200° and 25°C is presented in Fig. 4. As $YTaO_4$ or $MO_{1.5}$ composition increases, tetragonality increases in the ZrO_2–$YTaO_4$ system but it decreases in the ZrO_2–M_2O_3 system. The slope of tetragonality versus composition, as indicated under each curve, is smaller at 1200°C than at 25°C in both cases. The $t \to m$ transformation temperature in these two cases, measured by the dilatometric method, is suppressed as $MO_{1.5}$ or $YTaO_4$ composition increases. It implies that the $t \to m$ transformation temperature in the ZrO_2–$YTaO_4$ system decreases with increasing tetragonality, but it is reversed in the ZrO_2–M_2O_3.

Thermal expansion coefficients of the tetragonal phase versus its lattice constants are given in Fig. 5. The ordinate and the abscissa represent the average thermal expansion coefficients $(\alpha_a$ or $\alpha_c)$ in the two different crystallographic axes (c or a) at temperatures 900°–1200°C and the lattice constants (c or a) at

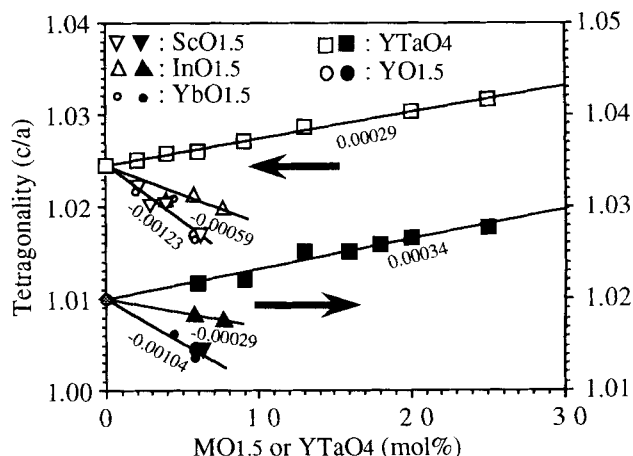**Fig. 2.** X-ray diffraction patterns of a 13.0 mol% $YTaO_4$ sample at three different temperatures.

Fig. 4. Tetragonality in the ZrO_2–$YTaO_4$ and ZrO_2–$MO_{1.5}$. Open symbols are for temperature at 1200°C and full symbols are for temperature at 25°C. Data under each curve is the slope of tetragonality versus composition.
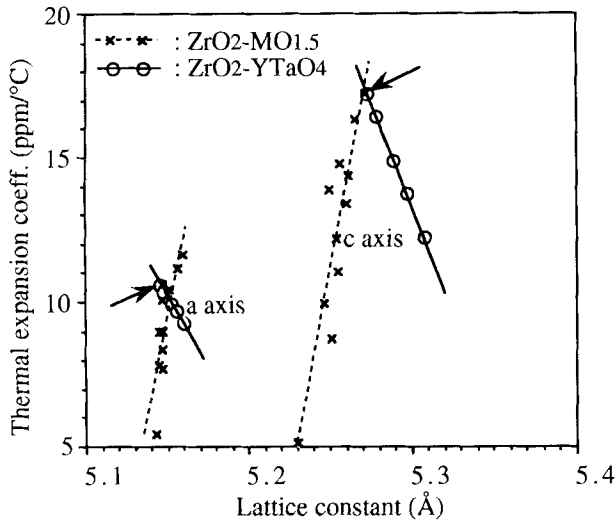
Fig. 5. Relationships between thermal expansion coefficient (α_c or α_a) and lattice constant (a or c). Arrows indicate data for pure ZrO_2.

1200°C, respectively. In ZrO_2–M_2O_3, α_a and α_c increase with increasing lattice constants. It is reversed in the ZrO_2–$YTaO_4$ system. For the crystallographic a direction, pure zirconia has the highest thermal expansion coefficient in ZrO_2–$YTaO_4$ but not in ZrO_2–M_2O_3. For the crystallographic c direction, pure zirconia has the highest thermal expansion coefficient in both systems. The anisotropic thermal expansion coefficient ratio (α_c/α_a) versus composition is shown in Fig. 6. α_c/α_a decreases with increasing $MO_{1.5}$ or $YTaO_4$ composition. Schubert's data at 25°–800°C for the ZrO_2–Y_2O_3 system[8] is close to ZrO_2–Yb_2O_3 in this study.

IV. Discussion

(1) Thermal Expansion in ZrO_2–Y_2O_3

Alderbert and Traverse[9] and Sheu *et al.*[10] have reported on the tetragonal phase (t or t') containing a temperature-dependent tetragonality, which first increases to a maximum and then decreases as temperature increases. Fundamentally, the t and t' phases are the same tetragonal polymorph in the zirconia solid
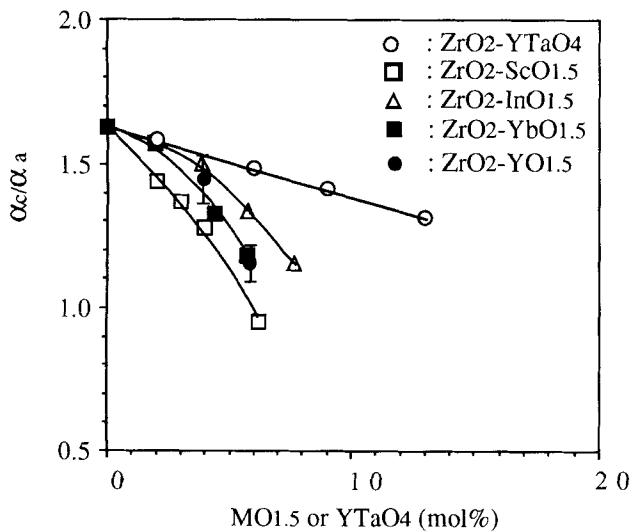
solutions.[10] Based on these previous data, the thermal expansion behavior of the tetragonal phase in the ZrO_2–Y_2O_3 system is discussed as follows.

There are two critical temperatures for each composition in this temperature-dependent tetragonality curve. One is at T_c, the transformation temperature of the cubic phase (c) to the tetragonal phase (t or t'). At T_c, the tetragonal phase shows a tetragonality anomaly, which decreases from $c/a \neq 1$ to $c/a = 1$.[9,10] This T_c temperature has been measured for the pure zirconia and the sample with 13.5 mol% $YO_{1.5}$. The other critical temperature is at T_a which has a maximum tetragonality $(c/a)_{max}$. At T_a, this temperature-dependent tetragonality ($c/a = f(T)$) has the following relationships: $f'(T) = 0$, and $f''(T) < 0$. Alternatively, $f'(T) = 0$ can be expressed as $\partial f(T)/\partial T = \partial(c/a)/\partial T = 0$. From $\partial(c/a)/\partial T = 0$, we obtain $(\partial c/\partial T) \times a - (\partial a/\partial T) \times c = 0$. Subsequently, $(\partial c/\partial T)/c = (\partial a/\partial T)/a$, i.e., $\alpha_c = \alpha_a$, is obtained at T_a. This derivation indicates that the tetragonal phase has the same thermal expansion coefficients in the crystallographic a and c directions when its tetragonality reaches a peak maximum, $(c/a)_{max}$.

Based on Alderbert's and Sheu's experimental data,[9,10] a ZrO_2–Y_2O_3 phase diagram containing $(c/a)_{max}$, $\alpha_c = \alpha_a$, $c/a = 1$, T_a, and T_c is shown in Fig. 7. Several published phase boundaries of the tetragonal and cubic phases[13–16] are also included. Symbols "*" are used to represent T_c temperatures. There are three data points for $c/a = 1$, at 25°, 600°, and 1200°C, respectively.[10] This $c/a = 1$ curve at high temperatures is close to one of the cubic phase boundaries.[16] Compared with the $c/a = 1$ curve, the $\alpha_c = \alpha_a$ or $(c/a)_{max}$ curve is very far from the cubic phase boundary. This locus of $\alpha_c = \alpha_a$ represents only a maximum tetragonality for the tetragonal phase, but not the phase boundary for the cubic phase. This is why the data point of $\alpha_c = \alpha_a$ does not match the cubic phase boundary in Schubert's paper.[8]

(2) Thermal Expansion in ZrO_2–M_2O_3 and ZrO_2–$YTaO_4$

By introducing the lattice constants from a linear regression method and the lattice constants of pure zirconia[3] at 25°C in ZrO_2–M_2O_3 and ZrO_2–$YTaO_4$, the average thermal expansion coefficients (α_c or α_a) of the tetragonal phase at 25°–1200°C versus its composition are shown in Fig. 8. For α_c, it decreases with increasing $MO_{1.5}$ or $YTaO_4$ composition. For α_a, it increases with increasing $MO_{1.5}$ composition (except for $ScO_{1.5}$) but decreases with increasing $YTaO_4$. Although thermal expansion coefficients (α_c and α_a) versus composition behave differently, the thermal expansion coefficient difference $\Delta\alpha$ ($= \alpha_c -$

Fig. 6. Thermal expansion coefficient ratio (α_c/α_a) versus composition in the temperature range 900°–1200°C. Data for ZrO_2–$YO_{1.5}$ are taken from Ref. 8.
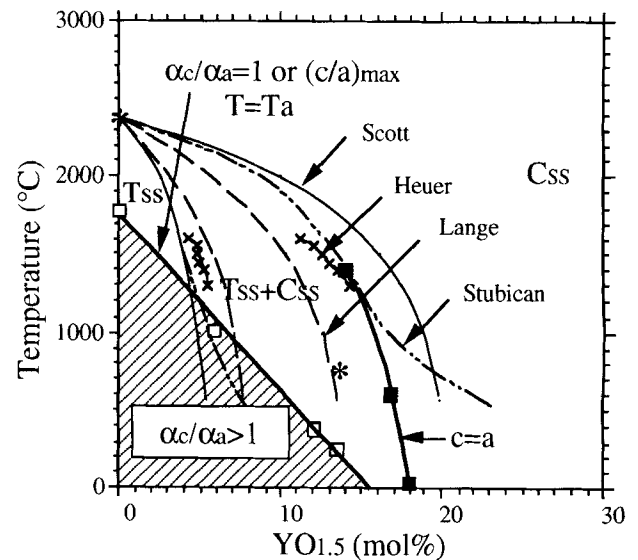

Fig. 7. Diagram showing the relationships among $\alpha_c/\alpha_a = 1$, $(c/a)_{max}$, and $c = a$. Tss is t-ZrO_2 solid solution, Css is c-ZrO_2 solid solution, T is temperature. Symbols "*" are for temperatures T_c.
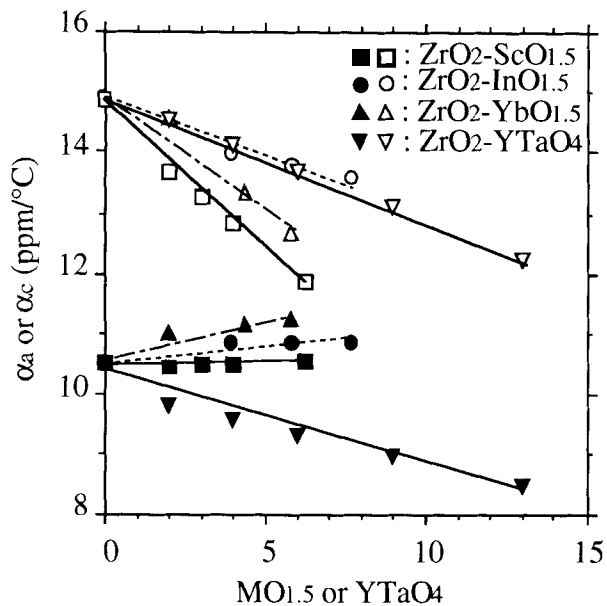
Fig. 8. Average thermal expansion coefficient at 25°–1200°C. Open symbols are for α_c and closed symbols are for α_a.

α_a) versus composition in these two systems shows the same trend, that is, it decreases with $MO_{1.5}$ or $YTaO_4$ composition. Compared with ZrO_2–Sc_2O_3 and ZrO_2–Yb_2O_3, ZrO_2–In_2O_3 and ZrO_2–$YTaO_4$ show a smaller change of $\Delta\alpha$ versus composition.

The relationships among the thermal expansion coefficient, the lattice constant, and composition in ZrO_2–$YTaO_4$ and ZrO_2–M_2O_3 are discussed as follows. For the thermal expansion coefficient (α_a or α_c) versus lattice constant (a or c) shown in Fig. 5, $(\partial\alpha_c/\partial c) > 0$ and $(\partial\alpha_a/\partial a) > 0$ in ZrO_2–M_2O_3, and $(\partial\alpha_c/\partial c) < 0$ and $(\partial\alpha_a/\partial a) < 0$ in ZrO_2–$YTaO_4$. For the lattice constant (c or a) versus composition (X) shown in Refs. 3 and 10 and in Fig. 3, $\partial c/\partial X < 0$ (except for M = Nd, when $\partial c/\partial X > 0$)[3] and $\partial a/\partial X > 0$ (except for M = Sc, when $\partial a/\partial X \le 0$)[10] in ZrO_2–M_2O_3, and $\partial c/\partial X > 0$ and $\partial a/\partial X > 0$ in ZrO_2–$YTaO_4$. From the above two relationships, it can be inferred that for the thermal expansion coefficient (α_a or α_c) versus composition (X), $(\partial\alpha_c/\partial X) < 0$ and $(\partial\alpha_a/\partial X) > 0$ in ZrO_2–M_2O_3 (except for M = Nd, Sc), and $(\partial\alpha_c/\partial X) < 0$ and $(\partial\alpha_a/\partial X) < 0$ in ZrO_2–$YTaO_4$. A schematic diagram to represent these relationships is given in Fig. 9. There exists $c = a$ in ZrO_2–M_2O_3, but not in ZrO_2–$YTaO_4$. $\alpha_c/\alpha_a = 1$ is present in both systems. By extrapolating data to $\alpha_c/\alpha_a = 1$ in Fig. 6, the locus of $\alpha_c = \alpha_a$ at 900°–1200°C in ZrO_2–M_2O_3 is approximately at 6 mol% $ScO_{1.5}$, 7 mol% $YbO_{1.5}$, and 9 mol% $InO_{1.5}$, respectively. This $\alpha_c/\alpha_a = 1$ is far from the cubic phase boundary in ZrO_2–M_2O_3. In ZrO_2–$YTaO_4$, the locus of $\alpha_c = \alpha_a$ is approximately at 25 mol% $YTaO_4$ at 900°–1200°C, even though the cubic phase does not exist in this system. This locus of $\alpha_c = \alpha_a$ is close to the tetragonal phase boundary at 900°–1200°C in ZrO_2–$YTaO_4$.
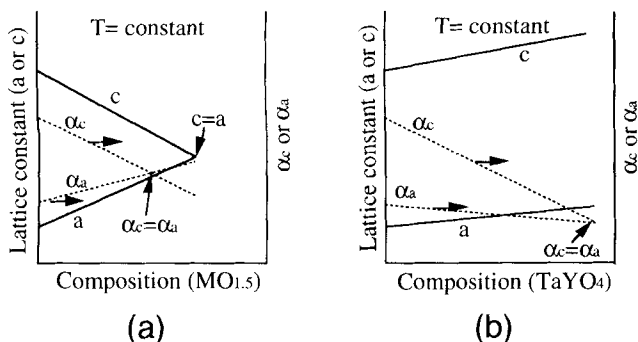

Fig. 9. Relationships among lattice constant, thermal expansion, and composition in the (a) ZrO_2–M_2O_3 and (b) ZrO_2–$YTaO_4$ systems.

Tetragonality is related to the magnitude of oxygen shear-type shifting in [001] {110}.[17] This oxygen shifting produces two different Zr–O bonds, four short ones and four long ones, for each Zr atom. In pure zirconia, Alderbert and Traverse[9] have found that the long Zr–O bond has a higher thermal expansion coefficient up to a certain temperature, and then it is reversed because this long Zr–O bond becomes unstable. This phenomenon causes the presence of $(c/a)_{max}$ or $\alpha_c = \alpha_a$ in the curve of tetragonality versus temperature. The presence of $\alpha_c = \alpha_a$ in the ZrO_2–M_2O_3 and ZrO_2–$YTaO_4$ systems suggests that the bond length change due to the effect of temperature in these two systems behaves like that in pure zirconia. However, why the thermal expansion coefficients of the tetragonal phase decrease with increasing lattice constants in the ZrO_2–$YTaO_4$ system is not fully understood.

(3) Thermal Stresses

In the tetragonal zirconia polycrystals, partially stabilized zirconia, and zirconia-toughened ceramic materials,[11,18–20] the thermal stresses from different kinds of mismatch (volume, expansion, etc.) have been shown to affect the transformability of tetragonal grains (or particles) in these materials. In the classical nucleation theory, the thermal stresses have accounted for the stress-induced transformation from the tetragonal (t) to the monoclinic (m) phase.[21,22] The anisotropic thermal expansion causes thermal stresses among differently orientated grains in the tetragonal zirconia polycrystals. Some grains are locally subjected to high thermal stresses. With increasing grain size, these thermal stresses are further increased up to the critical stresses to trigger the $t \rightarrow m$ transformation. In ZrO_2–M_2O_3 and ZrO_2–$YTaO_4$, the anisotropic thermal expansion coefficient difference ($\Delta\alpha = \alpha_c - \alpha_a$) in the two crystallographic axes of the tetragonal phase decreases with $MO_{1.5}$ or $YTaO_4$ content. Lower thermal stresses are expected to exist in the tetragonal polycrystals with a higher $MO_{1.5}$ or $YTaO_4$ content. As a result, the $t \rightarrow m$ transformation is more difficult to trigger by these thermal stresses.

Anisotropic thermal expansion is also temperature-dependent. A transition temperature T_a has been shown in Fig. 7. When $T < T_a$, then $\alpha_c > \alpha_a$; when $T > T_a$, then $\alpha_c < \alpha_a$. This reverse anisotropic thermal expansion behavior changes the magnitude of thermal stresses for the tetragonal zirconia polycrystals. For example, with the same grain size, tetragonal polycrystalline material being heat-treated above T_a and then quenched to the ambient temperature has lower thermal stresses than the sample being heat-treated at T_a. This is because the thermal stresses arising from cooling from T_a to the ambient temperature are relaxed by the reverse type of stresses arising from the heat-treating temperature T to T_a. Because of this characteristic curve of α_c/α_a versus temperature, a post-heat treatment just below temperature T_a for a long period of time is suggested to improve the transformability of the tetragonal polycrystals.

V. Conclusions

(1) From the lattice parameter measurements at high temperatures, a single tetragonal phase is determined to exist from 0–25 mol% $YTaO_4$ in the ZrO_2–$YTaO_4$ system. Its tetragonality (c/a) is larger than that in pure zirconia and increases with increasing $YTaO_4$ composition. However, with composition higher than 15 mol% $YTaO_4$, this tetragonal phase is stable at room temperature.

(2) Anisotropic thermal expansion coefficients of the tetragonal phase are measured at 25°–1200°C in ZrO_2–M_2O_3 and ZrO_2–$YTaO_4$. Thermal expansion coefficients, α_c and α_a, vary with M_2O_3 or $YTaO_4$ composition. However, the ratio and the difference of these two thermal expansion coefficients, α_c/α_a and $\alpha_c - \alpha_a$, decrease with increasing M_2O_3 or $YTaO_4$ composition, respectively.

(3) From the relationships among thermal expansion, temperature, and composition, the locus of $\alpha_c = \alpha_a$ exists in both

$ZrO_2-M_2O_3$ and ZrO_2-YTaO_4. This locus of $\alpha_c = \alpha_a$ indicates a maximum tetragonality $((c/a)_{max})$ for the tetragonal phase, but not the phase boundary for the cubic phase.

References

[1]M. Marezio, "Refinement of the Crystal Structure of In_2O_3 at Two Wavelengths," *Acta Crystallogr.*, **20**, 723–28 (1966).

[2]D. K. Hohnke, "Ionic Conductivity of $Zr_{1-2x}In_{2x}O_2$," *J. Phys. Chem. Solids*, **41**, 777–84 (1980).

[3]M. Yoshimura, "Phase Stability of Zirconia," *Am. Ceram. Soc. Bull.*, **67** [12] 1950–55 (1988).

[4]J. Lefevre, "Fluorite-Type Structural Phase Modification in Systems Having a Zirconium or Hafnium Oxide Base," *Ann. Chim. (Paris)* (in Fr.) **8** [1–2] 117–49 (1963); or translated by A. L. Monka, Report No. ORNL-TR-201.

[5]R. R. Lee, and A. H. Heuer, "Morphology of Tetragonal ZrO_2 in a Ternary (Mg,Y)-PSZ," *J. Am. Ceram. Soc.*, **70** [4] 208–13 (1987).

[6]D. J. Kim, "Effect of Ta_2O_5, Nb_2O_5, and HfO_2 Alloying on the Transformability of Y_2O_3-Stabilized Tetragonal ZrO_2," *J. Am. Ceram. Soc.*, **73** [1] 115–20 (1990).

[7]D. J. Kim, and T. Y. Tien, "Phase Stability and Physical Properties of Cubic and Tetragonal ZrO_2 in the System $ZrO_2-Y_2O_3-Ta_2O_5$," *J. Am. Ceram. Soc.*, **74** [12] 3061–65 (1991).

[8]H. Schubert, "Anisotropic Thermal Expansion Coefficients of Y_2O_3-Stabilized Tetragonal Zirconia," *J. Am. Ceram. Soc.*, **69** [3] 270–71 (1986).

[9]P. Alderbert, and J. P. Traverse, "Structure and Ionic Mobility of Zirconia at High Temperature," *J. Am. Ceram. Soc.*, **68** [1] 34–40 (1985).

[10]T. S. Sheu, T. Y. Tien, and I-W. Chen, "Cubic-to-Tetragonal (t') Transformation in Zirconia-Containing Systems," *J. Am. Ceram. Soc.*, **75** [5] 1108–16 (1992).

[11]A. H. Heuer, and M. Ruhle. "On the Nucleation of the Martensitic Transformation in Zirconia (ZrO_2)," *Acta Metall.*, **33** [12] 2101–12 (1985).

[12]T. A. Hahn, and R. K. Kirby, "Thermal Expansion of Platinum from 293 to 1900°K." Institute of Materials Research, National Bureau of Standards, Washington, DC, 1971.

[13]H. G. Scott, "Phase Relations in the Zirconia–Yttria System," *J. Mater. Sci.*, **10** [9] 1527–35 (1975).

[14]A. H. Heuer, and M. Ruhle, "Phase Transformations in ZrO_2-Containing Ceramics: I, The Instability of c-ZrO_2 and the Resulting Diffusion-Controlled Reactions"; pp. 1–13 in Advances in Ceramics, Vol. 12, *Science and Technology of Zirconia II*. Edited by N. Claussen, M. Ruhle, and A. H. Heuer. American Ceramic Society, Columbus, OH, 1984.

[15]F. F. Lange, "Transformation Toughening: Thermodynamic Approach to the Phase Retention and Toughening"; pp. 255–74 in *Fracture Mechanics of Ceramics*, Vol. 6. Edited by R. C. Bradt, A. G. Evans, D. P. H. Hasselmann, and F. F. Lange. Plenum Press, New York, 1983.

[16]V. S. Stubican, G. S. Corman, J. R. Hellmann, and G. Senft, "Phase Relationship in Some ZrO_2 Systems"; see Ref. 12, pp. 96–106.

[17]G. Teufer, "The Crystal Structure of Tetragonal ZrO_2," *Acta Crystallogr.*, **15**, 1187 (1962).

[18]R. C. Garvie and M. V. Swain, "Thermodynamics of the Tetragonal-to-Monoclinic Phase Transformation in Constrained Zirconia Microcrystals," *J. Mater. Sci.*, **20**, 1193–200 (1985).

[19]S. Schmauder, W. Mader, and M. Ruhle, "Calculations of Strain Distributions in and around ZrO_2 Inclusions"; see Ref. 14, pp. 251–55.

[20]A. H. Heuer, M. Ruhle, and D. B. Marshall, "On the Thermoelastic Martensitic Transformation in Tetragonal Zirconia," *J. Am. Ceram. Soc.*, **73** [4] 1084–93 (1990).

[21]I-W. Chen and Y. H. Chiao, "Martensitic Nucleation in ZrO_2," *Acta Metall.*, **31** [10] 1627–38 (1983).

[22]Y. H. Chiao, "Nucleation and Growth Processes of Martensitic Transformation in ZrO_2 Particles"; Ph.D. Thesis. Massachusetts Institute of Technology, Cambridge, MA, Sept. 1986. □